Journal of Hydroscience and Hydraulic Engineering
Vol. 20, No.1 May, 2002, 103-111

HYDRAULIC CHARACTERISTICS OF OPEN-CHANNEL FLOW DOWNSTREAM OF A DROP STRUCTURE WITH A TRENCH

By

I. FUJITA
Research Center for Urban Safety and Security, Kobe University, Kobe, Japan

and

T. MARUYAMA
Graduate Student, Graduate school of Kobe University, Kobe, Japan

SYNOPSIS

An open-channel turbulent flow downstream of a drop structure which has a trench in its downstream section was investigated experimentally by using image analysis methods. Two-dimensional flow field in a longitudinal cross-section illuminated by a laser-light-sheet was recorded by using a high-resolution video camera and visualized images were analyzed either by a particle tracking velocimetry (PTV) or by a particle image velocimetry (PIV) to investigate turbulent flow features for various trench aspect ratios. It was observed that the open-channel flow downstream of the drop structure reveals a drastic change in its flow pattern for a specific range of the trench aspect ratio; namely, a hydraulic jump created within the trench section periodically oscillates only for the specified range. The mechanism of the oscillation feature is also discussed in detail.

INTRODUCTION

In urban areas with hinterland that have steep slopes, such as in Kobe City, river channels are usuall.y made of concrete walls with rectangular cross-sections, and a number of drop structures have been constructed to decrease the energy slope of flow. In some cases, adding to a simple drop shape, a trench-shaped pool is installed in the downstream section of a drop structure to maintain a water surface within the pool even under very low flow conditions. Several examples of such a structure can be found in the downtown area of the Sumiyoshi River in Kobe City. The purpose of this supplementary structure is to provide people with a small water surface area within the trench (or a small waterfront environment), since, in such urban area, the normal flow rate is relatively very small and the river environment does not attract people to the river region. However, although the structure is instrumental in providing water front environments, it can generate unpredictable water surface deformation in case of floods due to the interaction of vortices produced at the trench with the water surface. Open-channel flows with a trench have been investigated by several researchers (e.g. Fujita, et al. (1,2), Nezu and Nakagawa (3) and Nezu et al. (4)), however, flow features associated with a trench section being subjected to a large water surface deformation have not been investigated so far. In this research, experiments utilizing image analysis techniques were carried out to examine the effects of the trench aspect ratio to the flow features such as water-surface patterns or turbulence structures.

EXPERIMENTS

Experimental Setup

The experiments were conducted using a 7.5m-length open-channel flume with a width of 0.30m. The bottom slope was kept constant at 1/500. Schematic of flow parameters at the trench section is depicted in Figure 1 and the hydraulic condition is shown in table 1. In the present experiment the length of the trench, L, was varied between 0.0cm and 11.0cm for the same hydraulic flow condition to examine the effect of the trench aspect ratio γ defined by L/dZ, where dZ is the difference of bed level between upstream and downstream channels. To visualize flow field by tracer particles, the flow was seeded by crashed nylon particles with a mean diameter of 60 μm and a specific gravity of 1.02. The image analysis system is shown in Figure 2. Images visualized by a laser-light sheet, emitted from an argon ion laser via a beam expander,

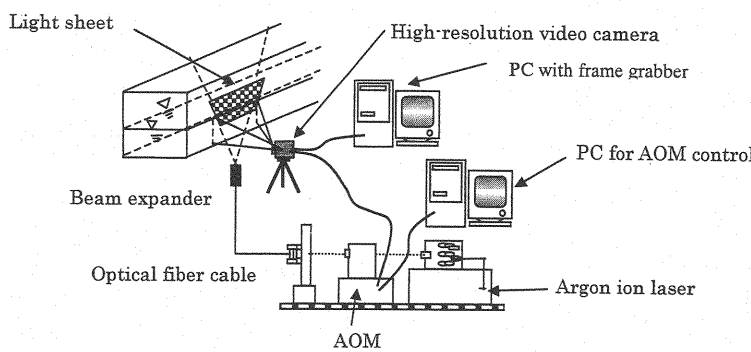

Fig.1 Image analysis system

Table 1 Hydraulic conditions

Q (m^3/s)	0.00227
Re	7590
Fr	0.889
Zd (cm)	1.0
Zu (cm)	2.0
Hd (cm)	1.95
U_1 (cm/s)	38.9
L (cm)	0.0 -11.0

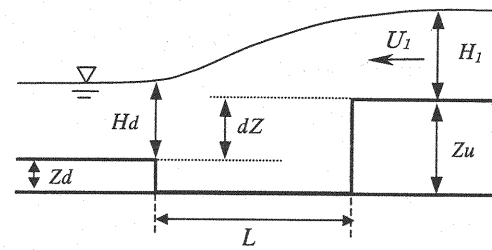

Fig.2 Schematic of flow parameters

are captured by a high-resolution video camera (Hitachi, KP-F100) with the image-sampling rate of 12 fps (frame per second). To freeze the tracer particle motion within a short time interval, a continuous laser light was chopped by means of an AOM (Acoustic Optical Modulator), yielding a pair of light pulses with a short time interval. In our experiment, the pulse interval, each having duration of 0.001 seconds, was set at 0.002 seconds so that the maximum tracer displacement becomes less than about ten pixels. In the present system, 162 consecutive images, cache with a size of 1304x1024 pixel, can be stored on a frame memory installed on a personal computer at one time. For each case, a total of 972 (=162x6) images (for about 81 seconds) were used to analyze turbulence characteristics at the trench section. The total amount of image data analyzed by PIV or PTV was about 19GB.

General Flow Patterns at the Trench Section

The flow feature downstream of a drop structure is subject to downstream water depth condition as well as to the trench aspect ratio. Figure 3(a) illustrates the schematic representation of flow patterns for the same downstream depth, in which the downstream water level was controlled so that a hydraulic jump is generated far downstream of a simple drop structure. As the trench length L increases, the hydraulic jump gradually changes its location towards upstream direction (Figure 3(b)) and finally reaches the trench section for the first critical trench length L_{C1} (or the first critical aspect ratio γ_{C1}). The movement of a hydraulic jump is attributed to the energy dissipation within the trench section, yielding a small increase of water depth just downstream of the trench, which also indicates a decrease of conjugate water depth that should occur nearer to the trench section in the downstream region of the hydraulic jump.

The hydraulic jump downstream of the trench and the flow within the trench exhibits almost steady flow feature until the hydraulic jump reaches the trench section. However, just after the hydraulic jump reaches the trench section, the free-surface pattern begins to change drastically from a steady state to an unstable one, accompanied by a periodic oscillation of a hydraulic jump within the trench section. This oscillation mode continues until the trench length reaches the second critical length, L_{C2} (or the second critical aspect ratio γ_{C2}). When we increase the trench length beyond L_{C2}, the flow pattern becomes stable again maintaining a steady hydraulic jump within the trench section.

The above description refers to the case in which a hydraulic jump is present downstream of the trench section; however, we found, in a further experimental study, that the oscillation phenomena actually occurs

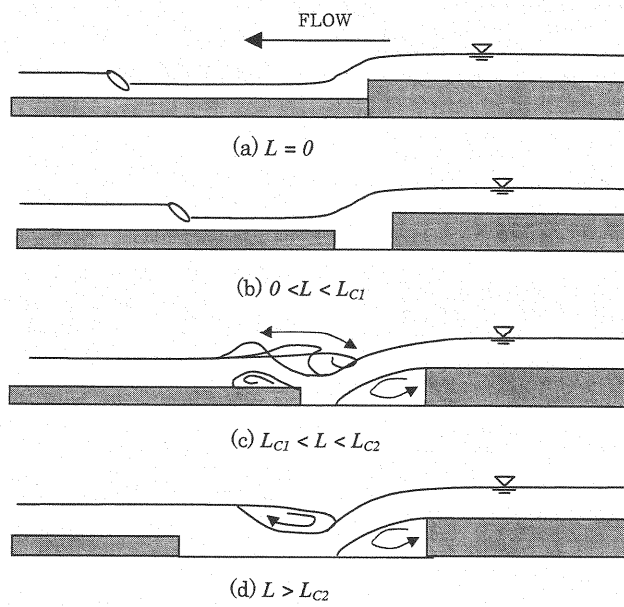

Fig.3 Variation of surface pattern with increasing trench length

irrespective of the presence of the downstream hydraulic jump as long as the specific condition for the trench aspect ratio is satisfied. Thus, in the present experiment, we started from the condition without a hydraulic jump in the downstream channel section. In the present case, the oscillation mode occurred for the aspect ratio between 6.5 and 9.0. This oscillating phenomenon is of great importance from the standpoint of the hydrodynamics because oscillation phenomena are rarely observed for other hydraulic conditions in a straight open channel flow.

Image Analysis Methods

In order to measure two-dimensional velocity distribution in a vertical cross section, we applied PTV (Particle Tracking Velocimetry) for non-oscillatory flows and PIV (Particle Image Velocimetry) for oscillatory flows, since PTV has a better spatial resolution than PIV and is more effective in measuring turbulence properties of highly shearing regions generated at the trench section. On the other hand, PIV is more robust to erroneous vectors that tend to increase for oscillatory flows. The erroneous vectors can be corrected by the correction algorithm for PIV proposed by the first author (Fujita and Kaizu (5)). In this research, the binarized cross correlation method was used as a PTV method and the cross correlation method was utilized as a PIV method. The template size for the pattern matching was 31x31 pixels for PTV, while its size was increased to 55x55 pixels for PIV in order to include more tracer particles within the template because the power of the laser light sheet was not strong enough for the video camera to detect all of the scattered light from tracer particles. The fluid region was separated from the aerial region by detecting the template location in which only the tracer particles were present, but more improvement is needed regarding the method of water-surface detection. When analyzing the PTV data, randomly distributed in space, each vector was picked up on a small flat mesh, 3.0mm by 1.0mm, assuming the uniformity of the flow property within the mesh.

RESULTS FOR NON-OSCILLATORY MODE

Mean Velocity Fields

As discussed previously, non-oscillatory flow pattern was generated for the aspect ratio less than 6.5 and greater than 9.0 for the present experimental conditions. Mean velocity distributions for this mode are

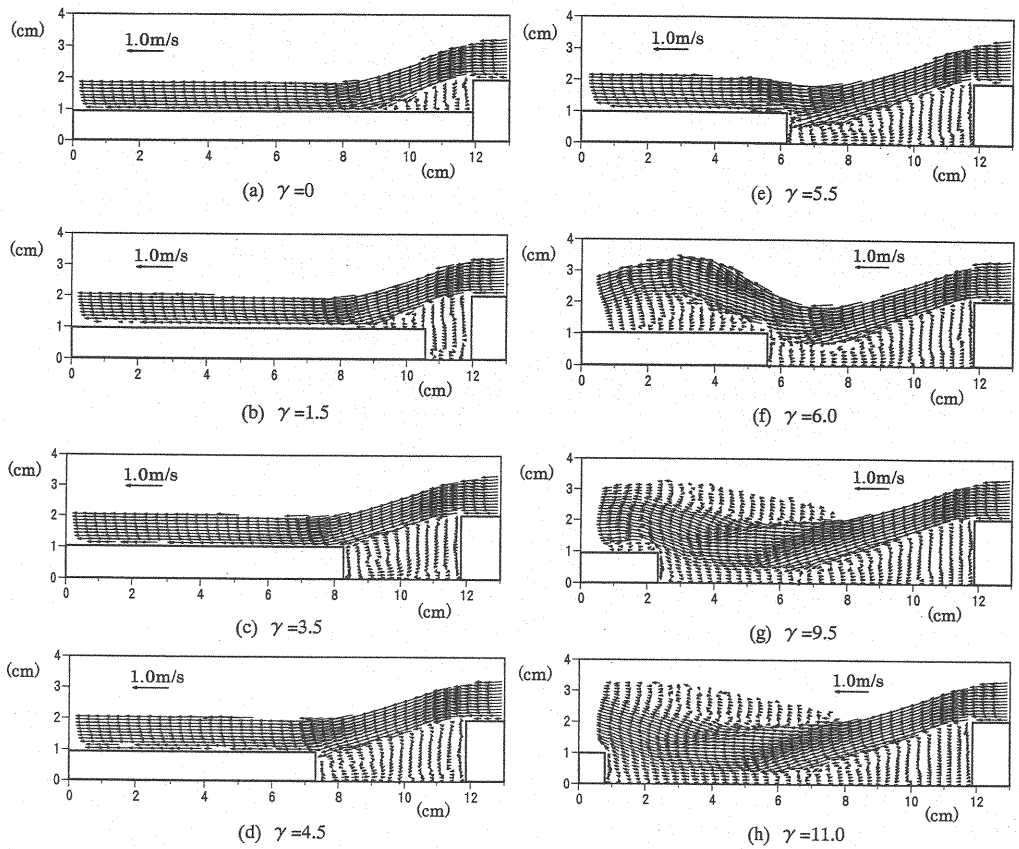

Fig.4 Mean velocity vectors obtained by PTV for non-oscillatory mode

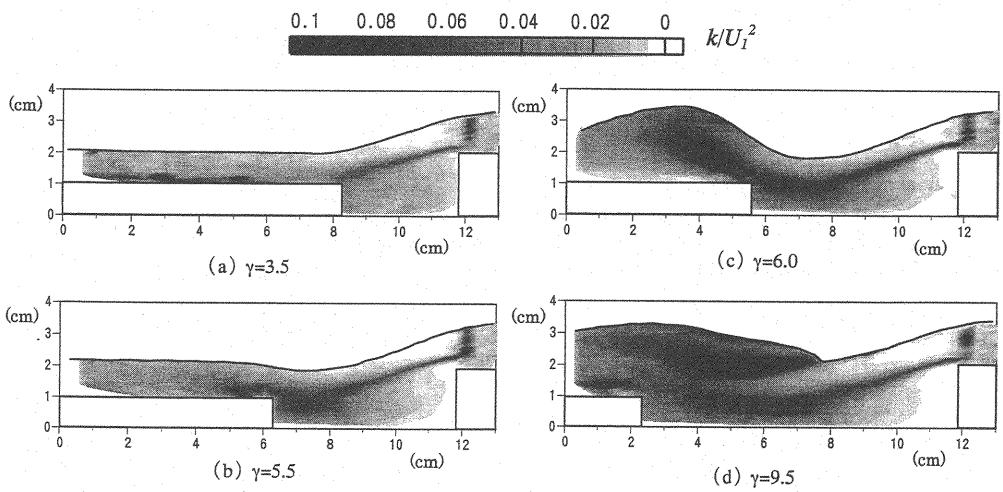

Fig.5 Distribution of turbulent kinetic energy

shown in Fig.4. Detailed flow structures are clearly obtained by the present PTV system. For the range of γ less than 3.5, the flow within the trench exhibits a cavity-like flow feature that accompanies a large

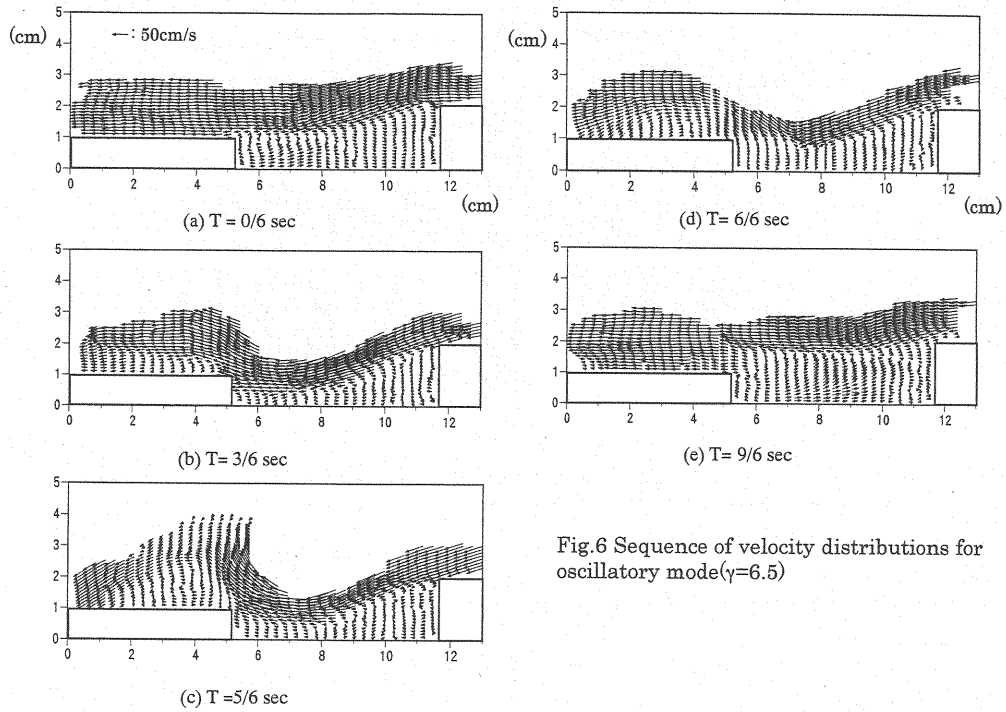

Fig.6 Sequence of velocity distributions for oscillatory mode(γ=6.5)

recirculating vortex with its center near the end of the trench. The water surface is connected smoothly to the downstream water level. When γ becomes 5.5, however, the lower part of the main flow begins to collide with the downstream trench wall, where velocity vectors have small upward components (Figure 4(e)). It should be noted that a small depression of the water surface is present near the end of the trench, which also suggest a sign of the interaction between the main flow and the downstream trench wall. For a little larger aspect ratio (γ=6.0), the direction of the main stream is completely deflected by the downstream trench wall and a new large separation zone is generated on the downstream side of the trench section, forming a wavy water surface configuration (Figure 4(f)). This condition is thought to be a neutrally stable (or a critical) state, because a slight increase of γ triggers a deformation of the wave-like water surface that tends to break down against the upstream direction. Once this breaking occurs it begins to oscillate periodically in a form of an oscillatory hydraulic jump. This phenomenon will be described in detail in the next section. This oscillatory mode persists while increasing γ up to 9.0.

When the aspect ratio becomes more than 9.0, the oscillating flow pattern ceases to occur and stable flow patterns are reproduced again as shown in Figures 4(g) and (h). In this case, the vertical width of the main stream entering the trench section gradually increases due to turbulent diffusion, while the main flow direction is deflected upward by the downstream trench wall. In addition, a stable roller (a steady hydraulic jump) is generated in the near-surface region; thereby the main stream submerges under the roller, forming a jet-like vertical velocity distribution within the trench section. It is interesting to note that the reattachment length, about 5.5cm in this case, corresponds to the trench length in which the interaction of the main flow with the downstream trench wall becomes evident, as mentioned previously in Figure 4 (e).

Turbulence properties

Turbulent kinetic energy distributions, k, for various aspect ratios are shown in Fig.5. The value of k is calculated from $k=(u'^2+2w'^2)/2$, where u' and w' are the turbulent intensities in the streamwise and vertical components, respectively. The local increase of k in the inlet section is due to the erroneous vectors. For the case of the smaller aspect ratio (γ=3.5), the shear layer created between the main flow and the cavity area rides smoothly on the downstream step (Figure 5 (a)), while, for a larger aspect ratio (γ=5.5), the collision of the main flow against the downstream trench wall creates a region with larger turbulent kinetic energy near the downstream part of the trench section (Figure 5(b)). When the aspect ratio becomes 6.0, due to the creation of a wave-shaped separation region downstream of the trench, a large amount of turbulence energy is generated along the newly developed shear layer in the downstream section as shown in Figure 5(c). For

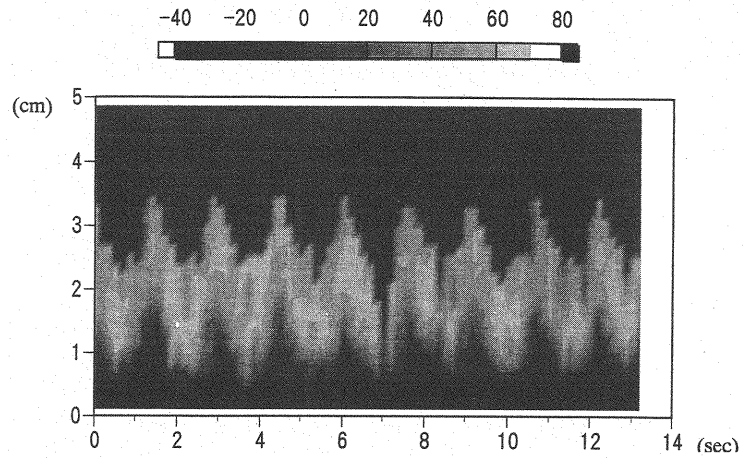

Fig.7 Time evolution of streamwise velocity distribution in a vertical cross section; at the section in the center of the trench for γ=6.5

the case of γ=9.5, a considerable amount of turbulence is produced along the boundary between the submerged main stream and the roller above the main flow as indicated in Figure 5(d). It should be noted that two parallel shear layers are present within the trench section in this case.

RESULTS FOR OSCILLATORY MODE

Instantaneous velocity field

Sequential velocity distributions for the case of γ=6.5 are shown in Figure 6. The insufficiency of velocity vectors in the upstream entering zone was due to the low illumination of a laser light sheet passing through the thick bottom wall with less transparency. The oscillation period was about 1.5 seconds. Obviously, the water surface is subject to a time-dependant large deformation, including generation and extinction of a hydraulic jump, within the trench section. It should be noted that the highest water level induced by the hydraulic jump instantaneously goes beyond the upstream water level which can be observed in Figure 6(c). Figure 6(d) demonstrates the flow pattern just after the breakdown of the hydraulic jump shown in Figure 6(c). Subsequently, a continuous supply of mass flux from the upstream main flow induces the increase of water volume within the trench section and flushes away the stagnant water volume created by the precedent breakdown of a hydraulic jump as shown in Figure 6(e). At this moment, the water surface becomes almost horizontal with a large recirculating flow within the trench section; however, this situation is no longer stable and another water surface deformation takes place again as indicated in Figure 6(f).

Time dependent feature

To demonstrate the periodic feature of the oscillating phenomenon, evolution of streamwise velocity distribution in a vertical cross-section in the center of the trench section was reproduced as a spatiotemporal image as shown in Figure 7. The upper dark area corresponds to the air-phase with no information on velocity, while the lower part indicates the fluid-phase with its velocity value represented by gray level color. This figure shows that a periodic oscillation is produced within the trench section whose influence goes deep into the bottom region.

Dependence on Reynolds number

In addition to the experiments presented herein, experiments for other geometric configuration were also conducted to investigate the general oscillation feature at the trench section. The relationship between the Strouhal number $St(=fdZ/U_1)$ and the Reynolds number $Re(=U_1dZ/\nu)$ is plotted in Figure 8, where f is the frequency of the oscillatory hydraulic jump. It can be seen that as the Reynolds number increases the

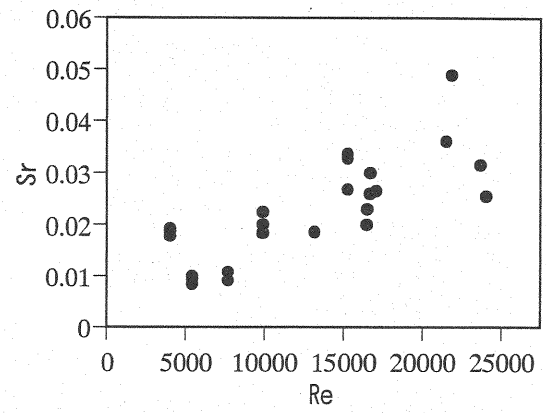

Fig.8 Frequency characteristics of oscillating hydraulic jump

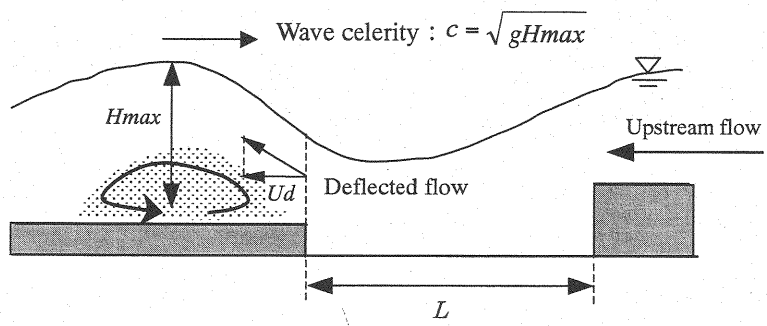

Fig.9 Schematic illustration of the balance between wave celerity and deflected flow

Strouhal number also increases despite some scatter in the plot. The cause of the scatter can be attributed to the fact that effect of the trench depth is not incorporated into the definition of the aspect ratio used in this paper. Further research is necessary to verify more general features of the oscillating phenomena.

Mechanism of the Oscillation

Figure 9 illustrates the flow pattern in the critical situation or in the neutrally stable condition. In this situation the flow deflected by the downstream step balances the celerity of the wave generated on the downstream side of the trench section; namely, streamwise component of the mean velocity at the downstream trench section, *Ud*, is almost the same as the wave celerity calculated from $c=(gHmax)^{1/2}$, where *Hmax* denotes the maximum wave height in the critical condition and g is the gravitational acceleration. For example, the flow condition shown in Figure 4(f) is close to this critical situation. In this case, *Ud* is about 51 cm/s while c is about 49.5cm/s using the observed maximum wave height 2.5cm. The fact that the wave celerity is a little less than *Ud* suggests that the created wave is incapable of traveling upstream against the mean flow. Another point to note concerning the critical situation is that there appears a large separation zone in the downstream section as illustrated in Figure 9. The size of this separation zone becomes larger as the downstream trench wall deflects the flow direction more upward, which eventually raises the maximum wave height resulting in the increase of its wave celerity. Hence, there should be a condition where the wave celerity becomes greater than *Ud*. When the condition is satisfied the wave begins to propagate upstream and finally it breaks down within the trench section. This wave breaking induces a hydraulic jump that is no longer stable and the sequence of flow oscillation is initiated as indicated in Figure 6.

CONCLUSION

In this study, open-channel turbulent flows downstream of a drop structure with a trench section were experimentally investigated with the aid of image analysis methods. It was demonstrated that two-dimensional variation of mean and turbulent flow properties could be measured fairly well by the present PTV and PIV systems. The remarkable feature of the flow in the presented configuration is that the surface flow pattern demonstrates a catastrophic change for a certain range of the trench aspect ratios; that is, an occurrence of an oscillating hydraulic jump within the trench section. The occurrence of the oscillating phenomenon can be explained qualitatively by a simple model but the general relationship between the trench aspect ratio and the oscillation frequency was not made clear theoretically in the present research. Furthermore, a more general geometric parameter that can include the influence of the trench depth needs to be investigated. Since the reproducibility of the oscillating phenomena is fairly good, the present results can be used to check the accuracy of the numerical simulation models that allows a large deformation and a breaking of free water surface.

AKNOWLEDGEMENT

This research was financially supported by the Grant-in-and for Scientific Research from the Japan Ministry of Education (Project No.12650514, Project leader: Ichiro Fujita).

REFERENCES

1. Fujita, I., Kanda, T. and Komura, S.: Measurements of turbulent flow in a trench using image processing technique, Proceedings 5th International Symposium on Refined Flow Modeling and Turbulence Measurements, pp.309-316, 1993.
2. Fujita, I., Kanda, T., Morita, T. and Kadowaki, M.: Numerical and image analysis of turbulent flow in open channel trench, HYDRA 2000, Vol.1, Thomas Telford, London, pp.284-289, 1995.
3. Nezu, I. and Nakagawa, H.: Turbulent structure of backward-facing step flow and coherent vortex shedding from reattachment in open channel flows, Turbulent Shear Flows, Vol.6, Springer-Verlag, pp.313-337, 1989.
4. Nezu, I., Yamamoto, Y. and Onitsuka, K.: Numerical simulation on turbulent structures in cavity flows by means of large eddy simulation, Annual Journal of Hydraulic Engineering, JSCE, Vol.42, pp.637-642, 1998. (in Japanese)
5. Fujita, I. and Kaizu, T.: Correction method of erroneous vectors in PIV, Journal of Visualization and Image Processing, Vol.2, pp.173-185, 1995.

APPENDIX – NOTATION

The following symbols are used in this paper:

C = wave celerity;
dZ = relative step height (= Zu - Zd);
f = frequency of hydraulic oscillation;
Fr = Froude number of the flow in the upstream section;
g = gravitational acceleration;
H_1 = upstream water depth;
Hd = water depth at the downstream trench section;
$Hmax$ = maximum water depth in the downstream section;
k = turbulent kinetic energy;
L = length of trench section;
L_{C1} = minimum trench length for hydraulic oscillation;
L_{C2} = maximum trench length for hydraulic oscillation;
Re = Reynolds number (= U_1H_1/ν);
Sr = Strouhal number(= fdZ/U_1);
u' = turbulent intensity of streamwise velocity component;

w' = turbulent intensity of vertical velocity component;
U_1 = mean velocity in upstream section;
Ud = streamwise component of mean velocity at downstream trench section;
Zu = height of upstream step;
Zd = height of downstream step;
γ = trench aspect ratio ($=L/dZ$); and
ν = kinematic viscosity.

(Received August 20, 2001 ; revised January 10, 2002)